Published in final edited form as:

FASEB J. 2023 September ; 37(9): e23133. doi:10.1096/fj.202201700RR.

Nuclear protein-1 is the common link for pathways activated by aging and obesity in chondrocytes: A potential therapeutic target for osteoarthritis

Li Tan[1], **Alexandra R. Armstrong**[2], **Samuel Rosas**[3], **Chirayu M. Patel**[4], **Sabrina S. Vander Wiele**[5], **Jeffrey S. Willey**[4], **Cathy S. Carlson**[2], **Raghunatha R. Yammani**[1]

[1]Section of Molecular Medicine, Department of Internal Medicine, Wake Forest University School of Medicine, Winston-Salem, North Carolina, USA

[2]Department of Veterinary Clinical Sciences, College of Veterinary Medicine, University of Minnesota, St. Paul, Minnesota, USA

[3]Department of Orthopaedic Surgery, Wake Forest University School of Medicine, Winston-Salem, North Carolina, USA

[4]Department of Radiation Oncology, Wake Forest University School of Medicine, Winston-Salem, North Carolina, USA

[5]Department of Biomedical Engineering, The College of New Jersey, Ewing Township, New Jersey, USA

Abstract

Pathways leading to osteoarthritis (OA) are diverse depending on the risk factors involved; thus, developing OA therapeutics has been challenging. Here we report that nuclear protein-1 (Nupr1), a stress-inducible protein/transcription factor, is activated by pathways associated with obesity and aging in chondrocytes. Treatment of human chondrocytes with free fatty acids (palmitate and oleate; a model for high-fat diet/obesity) induced PERK signaling and increased expression of caspase-3, TRB3, and Nupr1. On the other hand, treatment of chondrocytes with menadione (oxidative stress inducer) induced oxidation of IRE1, activated antioxidant response (higher Nrf2 expression), and increased expression of Nupr1 and matrix metalloproteinases. Experimental OA was induced by destabilization of the medial meniscus (DMM) in the knee joints of Nupr1$^{+/+}$ and

Correspondence Raghunatha R. Yammani, Section of Molecular Medicine, Department of Internal Medicine, Wake Forest University School of Medicine, Winston-Salem, NC 27157, USA. ryammani@wakehealth.edu.
Present address Li Tan, Department of Plastic and Reconstructive Surgery, Wake Forest University school of Medicine, Winston-Salem, North Carolina, USA

AUTHOR CONTRIBUTIONS

Li Tan conceived, designed, performed, and analyzed most of the experiments and wrote the manuscript; Alexandra R. Armstrong performed and analyzed the histology experiments; Samuel Rosas performed the DMM surgery; Chirayu M. Patel analyzed and interpreted the histology experiments and revised the manuscript; Chirayu M. Patel and Sabrina S. Vander Wiele analyzed and reconstructed the uCT images; Jeffrey S. Willey interpreted the uCT data; and Raghunatha R. Yammani conceived, designed, and supervised the study, analyzed and interpreted data, and wrote the manuscript. All authors reviewed and approved the final version of the manuscript.

DISCLOSURES

The authors declare that they have no conflict of interest.

SUPPORTING INFORMATION

Additional supporting information can be found online in the Supporting Information section at the end of this article.

Nupr1$^{-/-}$ mice. Loss of Nupr1 expression reduced the severity of cartilage lesions in this model. Together, our findings suggest that Nupr1 is a common factor activated by signaling pathways activated by obesity (ER stress) and age (oxidative stress) and a potential drug target for OA resulting from various risk factors.

Keywords

aging; cellular stress; Nupr1; obesity; osteoarthritis

1 | INTRODUCTION

Osteoarthritis (OA), the most common form of joint disease, causes persistent pain and physical disability and represents one of the most significant global healthcare burdens.[1] OA is a disease of the entire joint and is characterized by progressive loss of articular cartilage, synovitis, and bony changes.[2] About 27 million people are estimated to have OA in the US, and this number is expected to double by 2030.[3]

Obesity is one of the most widespread diseases globally and is a major risk factor for OA. Studies indicate a positive association between body weight/body mass index and the development of knee OA.[4,5] However, metabolic factors associated with obesity also play a critical role in the pathogenesis of OA.[6] We recently reported that high-fat diet (HFD)/obesity induces endoplasmic reticulum (ER) stress in joint tissues (cartilage and meniscus),[7-11] increases apoptosis,[8,9] and decreases cartilage matrix synthesis,[10] and autophagy.[11] Chondrocyte apoptosis plays an essential role in cartilage damage and the pathogenesis of OA.[12] Obesity is associated with elevated levels of free fatty acid,[13] resulting in lipotoxicity, cell dysfunction, inflammation, and cell death.[14] Accumulation of free fatty acid in joint tissues is associated with increased severity of cartilage lesions in OA.[15] We recently reported that feeding mice a diet supplemented with palmitate (saturated fatty acid) but not oleate (unsaturated fatty acid) induces ER stress to promote chondrocyte apoptosis and cartilage lesions in a mouse model of obesity-linked OA.[16]

Aging is another significant risk factor for OA. The prevalence of knee OA in individuals aged 45 and older rises with each decade of life from 14.9% in 45- to 54-year-olds to 49.9% in those over 75 years old.[17] Aging-related structural changes in human articular cartilage include cartilage thinning, lower glycosaminoglycan content,[18] altered cartilage proteoglycans, and accumulated advanced glycation end products.[19]

The chondrocyte is the only cellular component of articular cartilage. Its capacity to maintain protein homeostasis deteriorates with aging due to aging-linked cellular changes, including oxidative stress.[20] We recently found that age-associated decline in expression of molecular chaperones (e.g., calnexin) induces ER stress and chondrocyte apoptosis in articular cartilage of non-human primates, and knockdown of calnexin expression induces ER stress to promote chondrocyte apoptosis in human chondrocytes.[21]

Joint injury, most commonly to the anterior cruciate ligament (ACL), is an additional important risk factor for OA (also called post-traumatic OA) and accounts for about 12%

of all symptomatic cases.[22] Persons who suffer a previous knee injury are 4.2 times more likely to develop knee OA than those without a history of knee injury.[23] The underlying mechanism for injury-linked OA remains uncertain and appears to involve structural, biological, mechanical, and neuromuscular factors.[23] However, there is evidence that ER stress is involved in the development of injury-associated OA.[24]

Thus, OA is a multifactorial condition and its pathways could vary depending on the relevant risk factors. For example, emerging evidence demonstrates that the pathogenesis of aging-linked OA is different from that of injury-linked OA.[25] Thus, an ideal drug target would be involved in all types of OA development. We recently found that nuclear protein-1 (Nupr1), a stress-inducible transcription factor, is highly expressed in aged and osteoarthritic cartilage in humans and in dietary (HFD) and surgical (DMM surgery) models in mice,[7,21,26] making it a promising target candidate. In the present study, we show that Nupr1 is a crucial component in both obesity/HFD-ER stress and aging-oxidative stress pathways, although via different mechanisms. We further demonstrate that knockdown of Nupr1 expression inhibits palmitate-ER stress-mediated chondrocyte apoptosis and menadione-induced matrix metalloproteinase (MMP) production in vitro and significantly reduces the severity of cartilage lesions in a mouse model of injury-linked OA.

2 | MATERIALS AND METHODS

2.1 | Reagents and antibodies

The information for commercially available reagents and antibodies is provided in Tables S1 and S2.

2.2 | Chondrocyte isolation and culture conditions

Normal human cartilage tissues were obtained from the ankle joints of organ donors provided by the Gift of Hope Organ and Tissue Donor Network (Chicago, IL) through an agreement with Rush University Medical Center (Chicago, IL). Each cartilage specimen was graded for degenerative changes based on the 5-point Collins scale.[8] Only cells from tissue graded as 0 or 1 (indicating no symptom of arthritis) were used in experiments. All procedures and experimental protocols are approved by the Institutional Review Board (IRB) of the Wake Forest University School of Medicine. The authors did not have access to any identifiable information and, as noted in the IRB-approved protocol, no further consent was required. The ages of tissue donors ranged from 38 to 92 years.

Chondrocytes were isolated under aseptic conditions by sequential enzymatic digestion at 37°C using pronase at 2 mg/mL in serum-free Dulbecco's modified Eagle's medium/ Ham's F-12(1:1) (DMEMF)DMEM/F-12/antibiotics for 1 h, followed by overnight digestion with collagenase P at 0.36 mg/mL in DMEMF [5% fetal bovine serum (FBS)]. Viability of isolated cells was determined using trypan blue and cells were counted using a hemocytometer. Monolayer cultures were established by plating cells in six-well plates at 2 × 10^6 cells/well in DMEMF medium supplemented with 10% FBS at 37°C and 5% CO_2 for 1-2 days.

2.3 | Chondrocyte transfection

Chondrocytes were transfected by nucleofection using the Amaxa human chondrocyte nucleofector kit. Chondrocyte monolayers were treated with DMEMF/antibiotics containing 0.2% (w/v) pronase, 0.036% (w/v) collagenase P, and 10% (v/v) FBS for 3 h to detach the cells. Cells were collected by centrifugation (540× *g*, 10 min) and washed once with Dulbecco's phosphate-buffered saline (DPBS). They were then resuspended in the nucleofector solution containing siRNA (50 pmol/million cells), followed by transfection using program U-24 in the Amaxa Nucleofector II. After transfection, cells were immediately transferred into warmed DMEMF/antibiotics containing 20% (v/v) FBS in six-well plates previously coated with poly-lysine to help cell attachment, incubated at 37°C and 5% CO_2 overnight for recovery, then changed to DMEMF/antibiotics containing 10% (v/v) FBS overnight prior to cell treatment.

2.4 | Chondrocyte treatment

Palmitate and oleate were conjugated to fatty acid-free bovine serum albumin (BSA) as described previously.[8,9] For overnight treatment, chondrocyte monolayer cultures were changed to serum-free media for 6 h followed by treatments with either 25 μM of menadione, BSA alone (as a control), or 500 μM of BSA-conjugated palmitate or oleate at 37°C and 5% CO_2 overnight. For time course treatment, chondrocyte cultures were changed to serum-free media overnight followed by treatments with 25 μM of menadione as reported earlier[27] for 0, 15, 30, 60, 90, and 120 min, respectively. There was no reagent added at the 0-time point for menadione treatment. Inhibitors (e.g., 10 μM of p38i, 60 nM of 4μ8C 1 mM of PBA, or 1 nM of PERKi) were added into the cultures 1 h prior to the corresponding treatments as previously described.[9,20,21] After treatments, cells were washed with DPBS containing 1 mM phenylmethanesulfonyl fluoride solution (PMSF) and lysed with the cell lysis buffer containing 1 mM PMSF and 1/100 dilution of phosphatase inhibitor cocktail 2. For sulfenylation labeling, the cells were lysed with the above lysis buffer supplemented with 10 mM of N-ethylmaleimide, 10 mM of iodoacetamide, and 1 mM of BP1. The lysates were rotated on a tube rotator at 4°C for 30 min and then centrifuged (18 000× *g*, 10 min) at 4°C to remove any insoluble materials. Soluble proteins were quantified by the Micro BCA protein assay kit and stored at −20 or −80°C for future use. For measurement of MMP production, the conditioned medium was collected after the overnight treatment, supplemented with 1/100 dilution of NaN3 stock [5%(w/v)] to prevent potential contamination, and stored at 4°C for future use.

2.5 | Co-immunoprecipitation

Fifteen microliters of Dynabeads®-Protein A magnetic beads was vortexed and transferred to a centrifuge tube. The tube was placed on a magnet stand to separate the beads from the solution, and then the supernatant was removed. A quantity of 200 μL of antibody binding buffer [DPBS containing 0.02% (v/v) Tween-20] supplemented with 2 μL of anti-Nupr1 antibody was added into the tube followed by the rotation of the tube at room temperature for 15 min. The supernatant was removed after placing the tube on a magnet stand. The bead was then washed in 200 μL of antibody binding buffer and combined with 40 μg of chondrocyte lysate and incubated with rotation overnight at 4°C. The beads were

washed three times with 200 μL of DPBS and then eluted in 20 μL of elution buffer (50 mM Glycine, pH 2.8). The eluted sample was mixed with 5 μL of DPBS, 10 μL of 4× Laemmli's SDS-sample buffer, and 5 μL of 1 N NaOH and then heated at 100 °C in a heated block for 10 min for immunoblotting as follows. Immunoprecipitation of proteins from BP1-labeled samples was performed using Pierce™ streptavidin magnetic beads according to the manufacturer's instructions.

2.6 | Immunoblotting

Samples containing equal amounts of total proteins (or the same volume of conditioned medium) were reduced in 4× Laemmli's SDS-sample buffer and denatured at 100°C in a heated block for 10 min, separated by 10% sodium dodecyl sulfate-polyacrylamide gel electrophoresis, and transferred onto 0.45-μm nitrocellulose blotting membrane. The membranes were blocked with non-fat dry milk (5%, w/v) in 1× Tris-buffered saline-Tween-20 (TBST) for 1 h at room temperature with shaking, and were subsequently probed with primary antibodies at a predetermined optimal concentration in non-fat dry milk (5%, w/v in TBST) overnight with shaking at 4°C. The membranes were washed three times (5 min each) in TBST and then incubated with horseradish peroxidase (HRP)-conjugated secondary antibodies for 1 h at room temperature with shaking. Following three washings with TBST, the membranes were exposed to chemiluminescent HRP substrates (e.g., Amersham™ ECL, SuperSignal ELISA Pico, or Clarity Max™ western ECL subtract depending on signal intensity). Densitometry was performed on immunoblots using ImageJ software (National Institutes of Health). The data were expressed as relative band intensities normalized to internal loading controls (GAPDH except ADAMTS5 for conditioned medium). All immunoblotting experiments were repeated two to four times with cells obtained from independent donors.

2.7 | RNA isolation and quantitative real-time polymerase chain reaction (qRT-PCR)

Total RNA was isolated from the treated chondrocytes by the TRIzol method as described previously.[8] To synthesize complementary DNA, isolated total RNA (0.5–1 μg) was combined with 0.5 μg of random primers (Invitrogen) in 14 μL of RNase-free water, incubated at 70°C for 5 min, and then cooled immediately on ice. Two-hundred units of M-MLT reverse transcriptase (Promega) and dNTP Mix (2.5 mM) were then added into the RNA solution in a total volume of 25 μL of 1× reaction buffer (Promega), and incubated at 37°C for 60 min. Equivalent amounts of complementary DNA were used for real-time PCR in a 20-μL reaction mixture containing 10 μL of iTaq universal SYBR green supermix (Bio-Rad) and 1 μL of primer pairs specific for *nupr1, CHOP, TRB3*, or *TBP* (Qiagen). The qRT-PCR was performed using a 7500 Fast Real-Time PCR System (Applied Biosystems) and analyzed using 7500 Software v2.0.5 (Applied Biosystems) by the comparative CT method.[7] The expression level of targeted genes was normalized to TBP expression measured in parallel samples.

2.8 | Animal studies

Nupr1$^{-/-}$ mice were generated using a CRISPR-Cas9-mediated gene editing protocol by Horizon Discovery (St. Louis, MO). sgRNA targeting the first two-thirds of an open reading frame (consisting of exons 2 and 3, which represents 80% of the coding sequence of Nupr1)

of the Nupr1 gene was designed and assembled into a ribonucleoprotein complex with Cas9 endonuclease. The sgRNA was then delivered into zygotes from C57Bl/6 mice, followed by embryo transfer into pseudopregnant females. Transgenic founder animals were bred with C57BL/6 mice to produce F1 progeny heterozygous for Nupr1. Heterozygous $Nupr1^{+/-}$ mice were intercrossed to generate homozygous $Nupr1^{-/-}$ mice. Nupr1 deletion was confirmed by PCR-mediated genotyping, sequence analysis, and immunostaining. $Nupr1^{-/-}$ mice were of normal size, had normal phenotypes with no musculoskeletal deficiencies, and produced litters at a frequency consistent with Mend Elian inheritance.

All wild-type (WT; $Nupr1^{+/+}$ littermates) and $Nupr1^{-/-}$ mice ($n = 15$ per genotype) were housed in the Wake Forest University School of Medicine Vivarium under a 12-h dark/light cycle and were provided standard chow diet and water ad libitum. At 9 months of age, experimental OA was induced by DMM surgery in the left knee joints of mice.[28] A small cohort ($n = 5$ per genotype) of mice underwent sham surgery, in which the knee joint capsule was opened and closed without any further surgical procedure. After the surgical procedure, the mice were monitored closely for signs of apparent pain or adverse effects. Eight weeks after the DMM surgery, mice were sacrificed by CO_2 asphyxiation followed by cervical dislocation. Knee joints were fixed in 10% formalin, decalcified in Immunocal™, processed, and embedded in paraffin, and serially sectioned in the mid-coronal plane at a thickness of 4 μm. All experiments in mice were approved by the Wake Forest University School of Medicine Animal Care and Use Committee.

2.9 | Histology

Mid-coronal sections were stained with hematoxylin and eosin (H&E) and histologically assessed by two experienced evaluators who were blinded to group assignments. Mouse joint measurements were made using the OsteoMeasure histomorphometry system (OsteoMetrics) as previously described,[7] including articular cartilage area, articular cartilage area composed of dead chondrocytes, and an articular cartilage structure score (ACS). The ACS scores the integrity of the articular cartilage on a scale of 0-12, where 0 represents normal healthy cartilage and 12 represents full-thickness loss of the articular cartilage across more than two-thirds of the surface scored. Osteophytes were also graded as previously described[25] as follows: 0 = no osteophyte, 1 = small osteophyte, 2 = medium osteophyte, and 3 = large osteophyte. All histology scores for the medial tibial plateau are presented.

2.10 | Immunohistochemistry

Paraffin-embedded sections were deparaffinized in the xylene substitute Clear Advantage (Polysciences), rehydrated through a series of decreasing concentrations of ethanol, and washed with Tris-buffered saline (TBS). Antigens were retrieved with proteinase K treatment for 5 min. Sections were washed with TBS, treated with 3% hydrogen peroxide for 15 min, washed with TBS, blocked with Vectastain® goat normal serum for 15 min at room temperature, and incubated with a primary antibody (1:100 dilution for MMP3; 1:200 dilution for Nupr1; 1:500 dilution for CC3) in blocking serum overnight at 4°C. After washing with TBS, sections were incubated with biotinylated anti-rabbit secondary antibody for 30 min at room temperature, washed with TBS, and then incubated with Vectastain® Elite ABC reagent for 30 min at room temperature. Sections were again washed with TBS,

incubated with ImmPACT™ NovaRED™ peroxidase substrate (Vector Laboratories) for 5-30 min, washed with TBS, dehydrated and mounted, and then visualized using an Echo revolve fluorescence microscope. The following antibodies were used for immunohistochemistry: rabbit polyclonal anti-Nupr1 (bs-7106R from Bioss); rabbit monoclonal anti-CC3 (9664 from Cell Signaling Technology), and rabbit monoclonal anti-MMP3 (ab52915 from Abcam). At least three immunohistochemical images/regions containing 40-60 chondrocytes in the mouse knee cartilage were quantified using Adobe Photoshop CS6 (version 13.0) with correction for cell numbers.

2.11 | Contrast-enhanced micro-computed tomography

Cartilage thickness measures were quantified from reconstructed images after performing microCT as described previously.[29,30] Briefly, a subset of knees from 12-month-old $Nupr1^{-/-}$ and WT ($Nupr1^{+/+}$) mice ($n = 3$) were fixed in 10% neutral buffered formalin for 48 h, followed by storage in 70% ethyl alcohol. For contrast-enhanced imaging, each knee was submerged in 1% w/v phosphotungstic acid in 70% ethanol for a 24-h period prior to imaging using micro-computed tomography (SkyScan 1275), at 65 kV, 135 uA intensity, with isotropic voxels of 10 μm/side. Reconstructions were performed in Mimics v23 and analyzed to determine the location of the tibial-femoral cartilage-cartilage contact region of the medial tibial plateau, from which all measurements were performed. Cartilage thickness was measured at 15 different locations within this region and averaged per individual animal.

2.12 | Statistical analyses

Data are expressed as mean ± standard deviation. Statistical analyses were performed using GraphPad Prism 8 (version 8.2.0). For analyses of means of three or more groups, analysis of variance (ANOVA) tests were performed. If ANOVA results justified *post-hoc* comparisons between group means, the comparisons were conducted using Tukey's multiple comparison test. Two-tailed Student's *t*-tests were used for comparisons between the means of two groups as follows: non-parametric Mann–Whitney tests for ACS and osteophyte scores; unpaired *t*-tests for percentages of chondrocyte cell death, immunohistochemical data, and qRT-PCR data to compare age groups; and paired *t*-tests for quantifications of immunoblotting and the rest of the qRT-PCR data. The results were considered statistically significant at a value of $p < .05$. The precise *p* values have been provided wherever possible and appropriate.

3 | RESULTS

3.1 | Palmitate activates the PERK branch of UPR signaling and increases the expression of Nupr1 in human chondrocytes

To investigate which UPR signaling arm is involved in palmitate-mediated increased expression of Nupr1 in human chondrocytes, we used chemical inhibitors for PERK and IRE1, two of the prominent UPR signaling molecules. Pretreatment of chondrocytes with a PERK inhibitor (PERKi, GSK2606414) significantly reduced palmitate-induced expression of C/EBP homologous protein (CHOP), Nupr1, caspase 3 (CC3), and *tribbles* related protein-3 (TRB3), compared to an IRE1 inhibitor (4μ8C) (Figure 1A-E), indicating that

the PERK branch of UPR signaling is involved in palmitate-induced increased expression of Nupr1. NCBI human gene database analysis of the Nupr1 promoter revealed a putative binding site for ATF4 and CHOP (see Figure S1), suggesting that PERK/ATF4/CHOP could regulate Nupr1 expression transcriptionally in the palmitate-induced ER stress pathway in chondrocytes.

Inhibiting PERK signaling also reduced palmitate-induced TRB3 expression (Figure 1A,D), an anti-survival factor.[31] We found a putative binding site for Nupr1 on the human TRB3 promoter (see Figure S2). Nupr1 also regulates targeted protein function via protein-protein interactions.[32] Hence, we wanted to examine if Nupr1 interacts with TRB3 under palmitate-induced ER stress conditions. Our co-immunoprecipitation data demonstrated that Nupr1 is also associated with TRB3 (Figure 1F,I), suggesting that Nupr1 could regulate TRB3's expression transcriptionally and regulate its function via protein-protein interaction (Nupr1-TRB3 association) in palmitate-ER stress-induced apoptosis in chondrocytes.

3.2 | Oxidation of IRE1 induces Nupr1 and MMP production in human chondrocytes

To investigate how age-related mechanisms upregulate Nupr1 expression, we treated human chondrocytes with menadione, a potent oxidative stress inducer.[27] Menadione induced a rapid (30 min) and sustained increase in Nupr1 protein expression and increased phosphorylation of p-38 and IRE1 at Y628, but not autophosphorylation (S724) (Figures 2A and S3A,B,D). Menadione-induced activation of IRE1 increased expression of downstream signaling molecules, including spliced X-box binding protein 1 (XBP1s) and nuclear factor erythroid 2-related factor 2 (Nrf2), and caused increased phosphorylation of MAP kinase p38 (P-p38) (Figures 2A and S3C,E,F).

Since menadione induced IRE1 signaling, we wanted to examine if IRE1 is oxidized in chondrocytes. We assessed the oxidation of IRE1 using a biotin-linked dimedone derivative [biotin-1,3-cyclopentanedione (BP1)] molecule that interacts specifically with Cys-sulfenic acids (SOH), which are critical intermediates in redox signaling.[33-35] We observed that IRE1 was labeled with BP1 at 30 min (Figure 2B,C). Since sulfenylation is transient, it is not unusual to detect BP1-captured proteins at a single time point. We also observed increased phosphorylation of IRE1 (Y628) (Figures 2A and S3A), suggesting that phosphorylation and sulfenylation of IRE1 are two independent steps that regulate IRE1 function in oxidative stress in human chondrocytes.

Pretreatment of human chondrocytes with a potent and selective p38 inhibitor (p38i, SB202190) or IRE1 inhibitor (4μ8C) reduced the increased phosphorylation of IRE1 at Y628 and expression of XBP1s, Nupr1, and Nrf2 (Figures 2D and S3G,I-K), suggesting that p38 phosphorylates P-IRE1 at Y628 and induces the expression of XBP1, Nupr1, and Nrf2.

Similar data were obtained with overnight menadione treatment except that there was no significant change in p38 phosphorylation levels, suggesting that menadione-induced phosphorylation of MAP kinase p38 is transient (see Figure S4). Furthermore, treatment of chondrocytes with menadione induced increased production of MMP3 that correlated with increased phosphorylation of IRE1 at Y628 and increased expression of XBP1s and Nupr1 (see Figure S4A,B,D,E). MMP3 expression was inhibited by p38i (see Figure S4A,H)

and 4μ8C (Figure 2F), indicating that the p38/IRE1/Nupr1 pathway plays a crucial role in menadione-induced MMP3 in human chondrocytes.

To further study the role of Nupr1 in the oxidative stress pathway, we knocked down Nupr1 expression by siRNA and examined its effects on expression of XBP1s, Nrf2, MMP3, and phosphorylation of IRE1 (Y628). Using *nupr1*-specific siRNA, we reduced menadione-mediated Nupr1 induction by about 70% (Figures 2E and S5A). Knocking down Nupr1 expression reduced MMP3 expression but had no effect on expression of P-IRE1 (Y628), XBP1s, and Nrf2 (Figures 2E and S5B-E), indicating that Nupr1 is a downstream target molecule in the IRE1/XBP1s pathway.

Treatment of chondrocytes with menadione had no effect on expression of typical ER stress markers, including p-IRE1(S724), ATF4, CHOP, and cytochrome C; however, menadione induced increased phosphorylation of p- IRE1(Y628) and increased expression of XBP1s, Nupr1, Nrf2, and MMP3 (Figures 2F and S6). Pretreatment of chondrocytes with IRE-1 inhibitor (4μ8C) inhibited phosphorylation of IRE1 at Y628 and expression of XBP1s, Nupr1, Nrf2, and MMP3, but had no effect on ER stress markers [P-IRE1 (S724), ATF4, CHOP, and cytochrome C]. In contrast, pretreatment with 4-phenyl butyric acid, a general ER stress inhibitor,[36] had no effect on the phosphorylation of IRE1 (Y628) or any other molecules examined (Figures 2F and S6). These data demonstrate that menadione-induced oxidative stress is responsible for activation of the IRE1/XBP1s/Nupr1 pathway but not ER stress in human chondrocytes.

We also examined, if palmitate induces increased phosphorylation of IRE1 at Y628 in human chondrocytes, similar to menadione. However, treatment of chondrocytes with palmitate did not induce phosphorylation of IRE1 at Y628 or increase the expression of Nrf2, MMP3, or MMP13 (see Figure S7A,B,D,E,G). Furthermore, we also could not detect cysteine sulfenylation of IRE1 by palmitate. These results are consistent with previous findings showing that multiple ER stress inducers, including palmitate, have no effect on the ER redox state.[37] We found that palmitate-induced phosphorylation of p38 (see Figure S7A,E). However, the p38 inhibitor did not change expression of multiple ER stress-related proteins, including cytochrome C and CC3, which are activated downstream of the palmitate-ER stress pathway (see Figure S8). Our results suggest that although p38 was induced by palmitate via an unknown mechanism, it plays no role in palmitate-mediated ER stress.

3.3 | Menadione upregulates Nupr1 expression at the post-translational level

Our results demonstrate that both menadione and palmitate induce Nupr1 expression at the protein level. Hence, we wanted to test whether menadione also upregulates Nupr1 expression at the mRNA level. Surprisingly, menadione did not induce *nupr1* transcription at 2 h or overnight (Figures 3A and S9A), indicating that menadione does not regulate Nupr1 expression at the transcriptional level. Consistent with this result, menadione did not induce transcription of *CHOP* and *TRB3* (Figures 3B,C and S9B,C), whereas palmitate induced their transcription.[8]

However, menadione induced rapid phosphorylation of Nupr1 (Thr/Ser) as early as 15 min and, at the same time, reduced levels of Nupr1-associated ubiquitin (Figures 3D and S10A,B), suggesting that menadione upregulates Nupr1 protein levels by phosphorylation of Nupr1 and protects Nupr1 from ubiquitin/proteasome degradation. Furthermore, menadione-mediated phosphorylation of Nupr1 was inhibited by pretreatment of chondrocytes with p38i and 4μ8C (Figures 3E and S10C), suggesting that menadione regulates Nupr1 expression post-translationally via the p38/IRE1 pathway. In addition, NCBI human gene database analysis of the Nupr1 promoter showed a putative binding site for XBP1s (see Figure S11) and two putative binding sites for Nrf2 (see Figure S12). Together, our data demonstrate that Nupr1 could be regulated transcriptionally and post-translationally in response to menadione-mediated oxidative stress in chondrocytes.

3.4 | Aging promotes both ER stress and oxidative stress to promote chondrocyte apoptosis and matrix degradation in human articular cartilage

Chondrocytes isolated from aged (>60 years of age) human cartilage tissue showed increased phosphorylation of IRE1(Y628) and increased expression of Nrf2, MMP3, and MMP13 (Figure 4A,B,D,F) compared to chondrocytes from young donors (<50 years of age). However, we did not see increased phosphorylation of p38 with aging (Figure 4A,E), consistent with the effect of overnight menadione treatment (see Figure S4). Production of both MMP3 and MMP13 in the aged cells was inhibited by 4μ8C, but not by the ER stress inhibitors, PBA and PERKi (Figure 4F). Together, our data demonstrate that both ER stress and oxidative stress occur with aging and those pathways converge at Nupr1, which plays a major role in the pathogenesis of OA.

3.5 | Genetic deletion of Nupr1 diminishes the severity of cartilage lesions in a mouse model of post-traumatic OA

To investigate the critical role of Nupr1 in OA in vivo, we induced experimental OA by DMM surgery in the left knee joints of both wild-type (WT) ($Nupr1^{+/+}$) and $Nupr1^{-/-}$ mice. Histologic evaluation of sections stained with hematoxylin and eosin revealed less OA-like changes in the knee joints of $Nupr1^{-/-}$ mice compared to WT ($Nupr1^{+/+}$) (Figure 5A). Articular cartilage in $Nupr1^{-/-}$ mice showed less chondrocyte cell death (Figure 5B) and osteophyte formation (Figure 5C). Moreover, ACS scores were significantly lower in the joints of $Nupr1^{-/-}$ mice (mean severity of 4.07 ± 4.12 out of 12, $n = 14$) compared to WT ($Nupr1^{+/+}$) mice (mean severity of 10.23 ± 2.62 out of 12, $n = 13$) (Figure 5D). Furthermore, immunostaining of knee joints from $Nupr1^{-/-}$ mice confirmed *Nupr1* deletion and showed decreased expression of CC3, a biomarker for apoptosis, and MMP3 compared to WT mice (Figure 5F), indicating that Nupr1 plays a key role in chondrocyte apoptosis and cartilage matrix degradation in vivo. To examine if global deletion of Nupr1 has an effect on articular cartilage, we measured cartilage thickness in knee joints of $Nupr1^{-/-}$ and WT mice ($Nupr1^{+/+}$ littermates). We found no cartilage phenotype in the unchallenged mice (Figure 5E). Taken together, these results demonstrate that genetic deletion of Nupr1 significantly reduces the severity of cartilage lesions in a mouse model of injury-linked OA.

4 | DISCUSSION

Heterogeneity of the structural changes in OA is largely governed by its risk factors, including aging, obesity, and joint injury[6,17,22]; this heterogeneity creates a challenge for development of effective OA therapeutics. In the present study, we found that molecular pathways activated by aging, obesity, and joint injury all increased expression of the novel stress-inducible transcription factor, Nupr1 (albeit via different pathways). Nupr1 is involved in regulating chondrocyte apoptosis and causing increased production of MMPs (MMP-3 and 13), the major pathways associated with OA. In vitro knockdown of Nupr1 expression reduced obesity/HFD/palmitate-induced chondrocyte apoptosis[8] and oxidative stress/interleukin-1 induced increased production of MMPs.[26] Furthermore, genetic deletion of Nupr1 in mice reduced expression of apoptotic markers and MMPs in joint tissues and reduced severity of OA in our model of post-traumatic OA. Our studies demonstrate that Nupr1 plays a pivotal role in OA associated with aging, obesity, and joint injury (see Figure 6 for theoretical model), and thus could be an ideal target for treating all three types of OA.

Nupr1 is a versatile transcription factor induced by multiple stress stimuli, including inflammation and ER stress.[7,32] We reported earlier that oxidative stress and aging upregulated Nupr1 in cartilage/chondrocytes.[21,26] We recently reported that an age-dependent decline in calnexin protein, a molecular chaperone in chondrocytes, activated IRE1 signaling.[21] IRE1 is the primary arm of the ER stress/UPR signaling pathway. IRE1/UPR is activated via phosphorylation of the S724 (autophosphorylation site of IRE1) to restore cellular/ER homeostasis.[14] However, IRE1 is also involved in regulating the oxidative stress response.[38] This molecular switch occurs when IRE1 is oxidized by ROS.

The roles of IRE1 in UPR response and oxidative stress are mutually exclusive. That is, UPR signaling is turned off when responding to oxidative stress, and redox oxidative stress responses are turned off when responding to ER stress.[38] We found that menadione-induced oxidative stress did not change the autophosphorylation state of IRE-1 at S724; however, it increased the phosphorylation at Y628 that shifts IRE1's function from UPR signaling to oxidative stress. Thus, phosphorylation of IRE1 at Y628 acts as a molecular switch. Phosphorylation of IRE1 at the Y628 residue involves a so-called Tyr-down autoinhibitory mechanism in IRE1,[39] and mutations of the residue could affect the status of IRE1 autophosphorylation.[40] Autophosphorylation of the S724 residue is involved in the activation of IRE1 under ER stress/UPR signaling.[40] In contrast, our results suggest that p38 could mediate phosphorylation of the Y628 residue during oxidative stress. Hourihan et al.[38] reported that oxidation of IRE-1 activates expression of Nrf2, which regulates expression of an array of genes involved in the antioxidant response.[41] They also reported that IRE1's antioxidant response is regulated by cysteine sulfenylation. Cysteine sulfenylation, or the formation of cysteine sulfenic acid intermediates (Cys-SOH), is an oxidative post-translational modification involved in redox-dependent regulation of protein function.[42-44] Our data also showed that menadione-induced oxidation of IRE1 and formation of Cys-SOH coincided with increased phosphorylation at Y628 of IRE1, suggesting that phosphorylation and oxidation of IRE1 could independently or in conjunction regulate the antioxidative function of IRE1 in chondrocytes. We found a similar phenomenon in the regulation of c-Jun N-terminal kinase 2 activity in chondrocytes.[44]

Menadione induces increased phosphorylation of IRE1 (at Y628), coinciding with a rapid increase in Nrf2 and Nupr1 expression and increased production of MMP3 in human chondrocytes. Similarly, increased phosphorylation of IRE1 (at Y628) and increased expression/production of Nupr1, Nrf2, and MMPs were also observed in chondrocytes isolated from aged human cartilage. Inhibiting IRE1 activity or p38 activity blocked the oxidative stress-induced increased expression/production of Nrf2, Nupr1, and MMP3. However, we saw no effect of PBA, a general ER stress inhibitor, on menadione-induced phosphorylation (at Y628) of IRE1 and increased expression/production of Nrf2, Nupr1, and MMP3. Knocking down the expression of Nupr1 reduced menadione-mediated increased production of MMP3. Together, our data suggest that oxidative stress induces the oxidation of IRE1 to promote increased expression of Nupr1 and MMP production, but has no effect on the ER stress/UPR function of IRE1 in chondrocytes.

Menadione treatment of chondrocytes induced a rapid increase in protein levels of Nupr1; however, a similar increase in its mRNA was not observed, suggesting post-translational regulation of Nupr1. Nupr1 protein is labile and degrades rapidly via the proteasome/ubiquitin pathways, but phosphorylation of Nupr1 prevents its degradation.[45] We found that menadione treatment promoted phosphorylation of Nupr1 within 15 min and decreased ubiquitination. Thus, our data suggest that the rapid increase in Nupr1 protein levels in menadione-treated chondrocytes is due to phosphorylation-induced stability.

We recently reported that HFD/obesity induced increased expression of Nupr1 in cartilage tissue[7]; however, the mechanism involved was not clearly understood. Earlier, we reported that the saturated fatty acid palmitate induces ER stress and activates UPR signaling.[8] IRE1 and PERK are two important arms of the UPR signaling pathway that are activated by palmitate.[8] Our data showed that palmitate activated both PERK and IRE1 pathways in chondrocytes. We found increased phosphorylation of IRE1 at S724, the autophosphorylation site, but no phosphorylation of Y628, similar to the effects of menadione treatment. Blocking the PERK but not the IRE1 pathway inhibited palmitate-induced increased expression of CHOP, Nupr1, TRB3, and CC3, suggesting a dominant role of PERK in regulating Nupr1 expression in chondrocytes during obesity-induced ER stress. Activation of PERK recruits ATF4 and CHOP, a pro-apoptotic transcription factor.

We previously reported that knocking down CHOP expression in chondrocytes reduced palmitate-induced increased expression of Nupr1 and TRB3.[8] TRB3 is a pseudokinase that functions via protein-protein interactions; it binds Akt and regulates its function in cell survival pathways.[31] Knockdown of Nupr1 reduced palmitate-mediated increased expression of TRB3.[8] Sequencing database analyses of the Nupr1 promoter showed putative ATF4 and CHOP binding sites (see Figures S1), suggesting that these stress-inducible transcription factors play important roles in regulating Nupr1 expression under stress conditions. We also found a putative binding site for Nupr1 on the TRB3 promoter (see Figure S2) and that Nupr1 interacts with TRB3 during palmitate-induced ER stress, suggesting that Nupr1 is involved in regulating apoptosis and cell survival pathways. Together, our data suggest that the PERK/ATF4/CHOP pathway could play a major role in palmitate/HFD/obesity-induced expression of Nupr1.

We conclude that Nupr1 is a pivotal molecule upregulated by molecular pathways activated by aging, obesity, and joint injury for OA development, albeit via different pathways/mechanisms. Therefore, Nupr1 could be an ideal candidate for drug development to treat OA that results from diverse risk factors.

The study has some limitations; First, the role of Nupr1 was not analyzed in aged mice (spontaneous OA (aging) or in diet-induced obesity (obesity) mouse models to confirm its role in age and obesity-induced OA in vivo. Secondly, for our FFAs studies, we did not perform dose or time-course experiments for our analysis, especially to observe the changes in phosphorylation of IRE1 (Y628). Finally, for our DMM studies, we did not include young skeletally matured mice for our studies.

Supplementary Material

Refer to Web version on PubMed Central for supplementary material.

ACKNOWLEDGMENTS

This work was supported by the National Institute of Arthritis, Musculoskeletal and Skin Diseases (R01 AR066105) to R.R.Y. and by pilot funds from the Center for Redox Biology and Medicine (CRBM), Wake Forest University School of Medicine.

DATA AVAILABILITY STATEMENT

Data sharing is not applicable to this article, as no datasets were generated or analyzed during the current study.

Abbreviations:

DMM	destabilization of medial meniscus
ER	endoplasmic reticulum
HFD	high-fat diet
OA	osteoarthritis

REFERENCES

1. Cross M, Smith E, Hoy D, et al. The global burden of hip and knee osteoarthritis: estimates from the global burden of disease 2010 study. Ann Rheum Dis. 2014;73(7):1323–1330. [PubMed: 24553908]
2. Goldring SR, Goldring MB. Changes in the osteochondral unit during osteoarthritis: structure, function and cartilage-bone crosstalk. Nat Rev Rheumatol. 2016;12(11):632–644. [PubMed: 27652499]
3. Lawrence RC, Felson DT, Helmick CG, et al. Estimates of the prevalence of arthritis and other rheumatic conditions in the United States. Part II. Arthritis Rheum. 2008;58(1):26–35. [PubMed: 18163497]
4. Hootman JM, Helmick CG. Projections of US prevalence of arthritis and associated activity limitations. Arthritis Rheum. 2006;54(1):226–229. [PubMed: 16385518]
5. Oliveria SA, Felson DT, Cirillo PA, Reed JI, Walker AM. Body weight, body mass index, and incident symptomatic osteoarthritis of the hand, hip, and knee. Epidemiology. 1999;10(2):161–166. [PubMed: 10069252]

6. Berenbaum F, Eymard F, Houard X. Osteoarthritis, inflammation and obesity. Curr Opin Rheumatol. 2013;25(1):114–118. [PubMed: 23090672]
7. Tan L, Harper L, McNulty MA, Carlson CS, Yammani RR. High-fat diet induces endoplasmic reticulum stress to promote chondrocyte apoptosis in mouse knee joints. FASEB J. 2020;34(4):5818–5826. [PubMed: 32124494]
8. Tan L, Yammani RR. Nupr1 regulates palmitate-induced apoptosis in human articular chondrocytes. Biosci Rep. 2019;39(2):BSR2018473.
9. Haywood J, Yammani RR. Free fatty acid palmitate activates unfolded protein response pathway and promotes apoptosis in meniscus cells. Osteoarthr Cartil. 2016;24(5):942–945.
10. Nazli SA, Loeser RF, Chubinskaya S, Willey JS, Yammani RR. High fat-diet and saturated fatty acid palmitate inhibits IGF-1 function in chondrocytes. Osteoarthr Cartil. 2017;25(9):1516–1521.
11. Mallik A, Yammani RR. Saturated fatty acid palmitate negatively regulates autophagy by promoting ATG5 protein degradation in meniscus cells. Biochem Biophys Res Commun. 2018;502(3):370–374. [PubMed: 29852167]
12. Thomas CM, Fuller CJ, Whittles CE, Sharif M. Chondrocyte death by apoptosis is associated with the initiation and severity of articular cartilage degradation. Int J Rheum Dis. 2011;14(2):191–198. [PubMed: 21518319]
13. Opie LH, Walfish PG. Plasma free fatty acid concentrations in obesity. N Engl J Med. 1963;268:757–760. [PubMed: 13940209]
14. Hotamisligil GS. Endoplasmic reticulum stress and the inflammatory basis of metabolic disease. Cell. 2010;140(6):900–917. [PubMed: 20303879]
15. Lippiello L, Walsh T, Fienhold M. The association of lipid abnormalities with tissue pathology in human osteoarthritic articular cartilage. Metabolism. 1991;40(6):571–576. [PubMed: 1865821]
16. Tan L, Harper LR, Armstrong A, Carlson CS, Yammani RR. Dietary saturated fatty acid palmitate promotes cartilage lesions and activates the unfolded protein response pathway in mouse knee joints. PLoS One. 2021;16(2):e0247237. [PubMed: 33617553]
17. Jordan JM, Helmick CG, Renner JB, et al. Prevalence of knee symptoms and radiographic and symptomatic knee osteoarthritis in African Americans and Caucasians: the Johnston County Osteoarthritis Project. J Rheumatol. 2007;34(1):172–180. [PubMed: 17216685]
18. Roughley PJ, White RJ. Age-related changes in the structure of the proteoglycan subunits from human articular cartilage. J Biol Chem. 1980;255(1):217–224. [PubMed: 7350154]
19. DeGroot J, Verzijl N, Bank RA, Lafeber FP, Bijlsma JW, TeKoppele JM. Age-related decrease in proteoglycan synthesis of human articular chondrocytes: the role of nonenzymatic glycation. Arthritis Rheum. 1999;42(5):1003–1009. [PubMed: 10323457]
20. Loeser RF, Gandhi U, Long DL, Yin W, Chubinskaya S. Aging and oxidative stress reduce the response of human articular chondrocytes to insulin-like growth factor 1 and osteogenic protein 1. Arthritis Rheumatol. 2014;66(8):2201–2209. [PubMed: 24664641]
21. Tan L, Register TC, Yammani RR. Age-related decline in expression of molecular chaperones induces endoplasmic reticulum stress and chondrocyte apoptosis in articular cartilage. Aging Dis. 2020;11:1091–1102. [PubMed: 33014525]
22. Brown TD, Johnston RC, Saltzman CL, Marsh JL, Buckwalter JA. Posttraumatic osteoarthritis: a first estimate of incidence, prevalence, and burden of disease. J Orthop Trauma. 2006;20(10):739–744. [PubMed: 17106388]
23. Muthuri SG, McWilliams DF, Doherty M, Zhang W. History of knee injuries and knee osteoarthritis: a meta-analysis of observational studies. Osteoarthr Cartil. 2011;19(11):1286–1293.
24. Tang YH, Yue ZS, Zheng WJ, et al. 4-Phenylbutyric acid presents therapeutic effect on osteoarthritis via inhibiting cell apoptosis and inflammatory response induced by endoplasmic reticulum stress. Biotechnol Appl Biochem. 2018;65(4):540–546. [PubMed: 29327364]
25. Rowe MA, Harper LR, McNulty MA, et al. Reduced osteoarthritis severity in aged mice with deletion of macrophage migration inhibitory factor. Arthritis Rheumatol. 2017;69(2):352–361. [PubMed: 27564840]
26. Yammani RR, Loeser RF. Brief report: stress-inducible nuclear protein 1 regulates matrix metalloproteinase 13 expression in human articular chondrocytes. Arthritis Rheumatol. 2014;66(5):1266–1271. [PubMed: 24497499]

27. Collins JA, Wood ST, Nelson KJ, et al. Oxidative stress promotes peroxiredoxin hyperoxidation and attenuates prosurvival signaling in aging chondrocytes. J Biol Chem. 2016;291(13):6641–6654. [PubMed: 26797130]
28. Glasson SS, Blanchet TJ, Morris EA. The surgical destabilization of the medial meniscus (DMM) model of osteoarthritis in the 129/SvEv mouse. Osteoarthr Cartil. 2007;15(9):1061–1069.
29. Kwok AT, Moore JE, Rosas S, et al. Knee and hip joint cartilage damage from combined spaceflight hazards of low-dose radiation less than 1 Gy and prolonged hindlimb unloading. Radiat Res. 2019;191:497–506. [PubMed: 30925135]
30. Kwok AT, Mohamed NS, Plate JF, et al. Spaceflight and hind limb unloading induces an arthritic phenotype in knee articular cartilage and menisci of rodents. Sci Rep. 2021;11:10469. [PubMed: 34006989]
31. Ohoka N, Yoshii S, Hattori T, Onozaki K, Hayashi H. TRB3, a novel ER stress-inducible gene, is induced via ATF4-CHOP pathway and is involved in cell death. EMBO J. 2005;24(6):1243–1255. [PubMed: 15775988]
32. Goruppi S, Iovanna JL. Stress-inducible protein p8 is involved in several physiological and pathological processes. J Biol Chem. 2010;285(3):1577–1581. [PubMed: 19926786]
33. Paulsen CE, Carroll KS. Cysteine-mediated redox signaling: chemistry, biology, and tools for discovery. Chem Rev. 2013;113(7):4633–4679. [PubMed: 23514336]
34. Furdui CM, Poole LB. Chemical approaches to detect and analyze protein sulfenic acids. Mass Spectrom Rev. 2014;33(2):126–146. [PubMed: 24105931]
35. Nelson KJ, Klomsiri C, Codreanu SG, et al. Use of dimedone-based chemical probes for sulfenic acid detection methods to visualize and identify labeled proteins. Methods Enzymol. 2010;473:95–115. [PubMed: 20513473]
36. Ozcan U, Yilmaz E, Ozcan L, et al. Chemical chaperones reduce ER stress and restore glucose homeostasis in a mouse model of type 2 diabetes. Science. 2006;313(5790):1137–1140. [PubMed: 16931765]
37. Schuiki I, Zhang L, Volchuk A. Endoplasmic reticulum redox state is not perturbed by pharmacological or pathological endoplasmic reticulum stress in live pancreatic beta-cells. PLoS One. 2012;7(11):e48626. [PubMed: 23144914]
38. Hourihan JM, Moronetti Mazzeo LE, Fernandez-Cardenas LP, Blackwell TK. Cysteine sulfenylation directs IRE-1 to activate the SKN-1/Nrf2 antioxidant response. Mol Cell. 2016;63(4):553–566. [PubMed: 27540856]
39. Joshi A, Newbatt Y, McAndrew PC, et al. Molecular mechanisms of human IRE1 activation through dimerization and ligand binding. Oncotarget. 2015;6(15):13019–13035. [PubMed: 25968568]
40. Prischi F, Nowak PR, Carrara M, Ali MM. Phosphoregulation of Ire1 RNase splicing activity. Nat Commun. 2014;5:3554. [PubMed: 24704861]
41. Vomund S, Schafer A, Parnham MJ, Brune B, von Knethen A. Nrf2, the master regulator of anti-oxidative responses. Int J Mol Sci. 2017;18(12):2772. [PubMed: 29261130]
42. Klomsiri C, Karplus PA, Poole LB. Cysteine-based redox switches in enzymes. Antioxid Redox Signal. 2011;14(6):1065–1077. [PubMed: 20799881]
43. Roos G, Messens J. Protein sulfenic acid formation: from cellular damage to redox regulation. Free Radic Biol Med. 2011;51(2):314–326. [PubMed: 21605662]
44. Nelson KJ, Bolduc JA, Wu H, et al. H_2O_2 oxidation of cysteine residues in c-Jun N-terminal kinase 2 (JNK2) contributes to redox regulation in human articular chondrocytes. J Biol Chem. 2018;293(42):16376–16389. [PubMed: 30190325]
45. Goruppi S, Kyriakis JM. The pro-hypertrophic basic helix-loop-helix protein p8 is degraded by the ubiquitin/proteasome system in a protein kinase B/Akt- and glycogen synthase kinase-3-dependent manner, whereas endothelin induction of p8 mRNA and renal mesangial cell hypertrophy require NFAT4. J Biol Chem. 2004;279(20):20950–20958. [PubMed: 15016802]

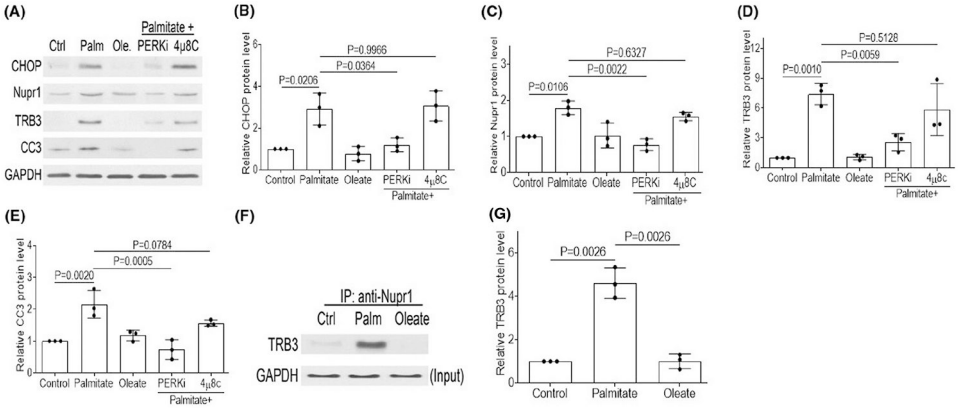

FIGURE 1.

Palmitate activates the PERK branch of UPR signaling and increases the expression of Nupr1 in human chondrocytes. (A) Human chondrocytes were stimulated with 500 μM BSA-conjugated palmitate or oleate overnight and probed for CHOP, Nupr1, TRB3, and CC3 antibodies, respectively. Inhibitors (1 nM of PERKi or 60 nM of 4μ8C) were added to the cells 1 h prior to the treatments as needed. Blots were stripped and reprobed with GAPDH as a loading control. Densitometric analyses for protein levels of CHOP (B), Nupr1 (C), TRB3 (D), and CC3 (E) were performed on blots obtained in three independent experiments similar to the one shown in panel A. (F) Human chondrocytes were stimulated with 500 μM BSA-conjugated palmitate or oleate overnight. The protein lysates obtained were assessed by co-immunoprecipitation with a Nupr1-specific antibody, and the Nupr1-associated proteins were then probed for TRB3 antibody. Densitometric analyses for protein levels of TRB3 (G) were performed on blots obtained from three independent experiments similar to the one shown in panel F. Data are shown as mean ± standard deviation of the mean. Ctrl, Control; Palm, Palmitate; Ole., Oleate.

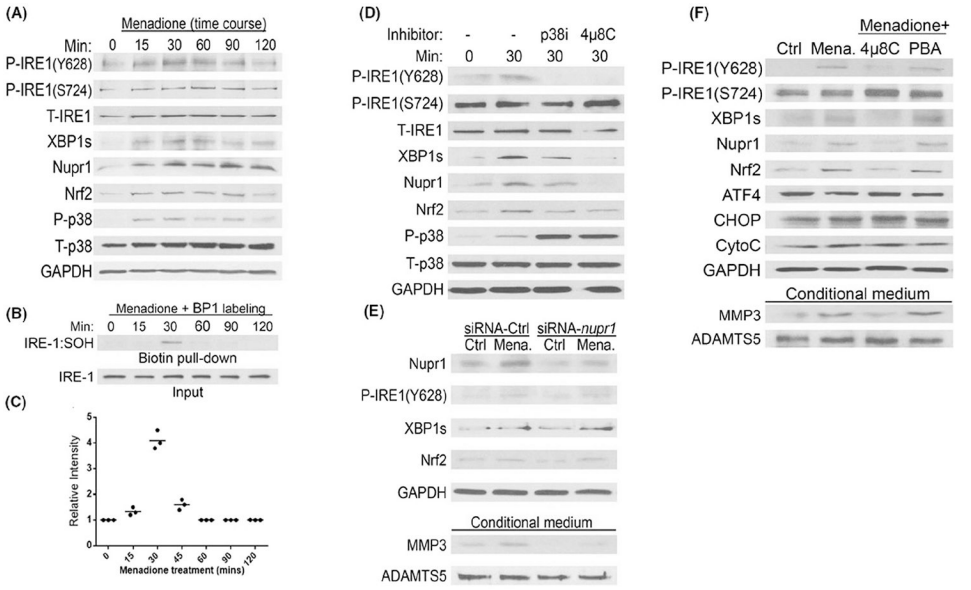

FIGURE 2.

Oxidation of IRE1 induces Nupr1 and MMP production in human chondrocytes. (A) Human chondrocytes were treated with 25 μM of menadione for 0, 15, 30, 60,90, and 120 min, respectively, and probed for P-IRE1(Y628 or S724), total IRE1(T-IRE1), XBP1s, Nupr1, Nrf2, P-p38, and total p38 (T-p38) antibodies, respectively. (B) Human chondrocytes treated with 25 μM of menadione for 0-120 min were assessed for IRE-1:SOH by immunoblot. Densitometric analyses for protein levels of IRE-1:SOH (C) were performed on blots obtained from three independent experiments similar to the one shown in panel B. Data are shown as mean ± standard deviation of the mean. (D) Human chondrocytes were treated with 25 μM of menadione for 0 and 30 min, and probed for P-IRE1(Y628 or S724), T-IRE1, XBP1s, Nupr1, Nrf2, P-p38, and T-p38 antibodies, respectively. Inhibitors (10 μM of p38i or 60 nM of 4μ8C were added to the cells 1 h prior to the treatments as needed. (E) Human chondrocytes were transfected with control siRNA or siRNA specific for *nupr1*, and then treated with 25 μM of menadione overnight and probed for Nupr1, P-IRE1 (Y628), XBP1s, and Nrf2, respectively. Conditioned medium was probed for MMP3 and ADAMTS5. (F) Human chondrocytes were treated with 25 μM of menadione overnight and probed for P-IRE1(Y628 or S724), XBP1s, Nupr1, Nrf2, ATF4, CHOP, and cytochrome C (CytoC) respectively. Conditioned medium was probed for MMP3 and ADAMTS5. Inhibitors (60 nM of 4μ8C or 1 mM of PBA) were added into the cells 1 h prior to the treatments as needed. Blots were stripped and reprobed with GAPDH as a loading control. For conditioned medium, blots were stripped and reprobed with ADAMTS5 as a loading control.

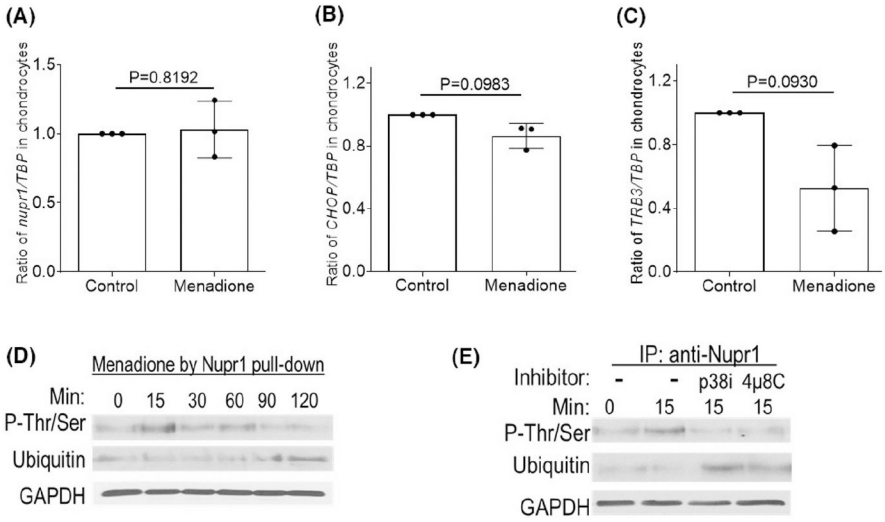

FIGURE 3.

Menadione upregulates Nupr1 expression at the post-translational level. Human chondrocytes were treated with 25 μM of menadione overnight; total RNA was isolated, cDNA was synthesized, and qRT-PCR was performed using primers specific for *nupr1* (A), *CHOP* (B), and *TRB3* (C). Data were normalized to TBP as a control and shown as mean ± standard deviation of the mean ($n = 3$). (D) Human chondrocytes were treated with 25 μM of menadione for 0, 15, 30, 60,90, and 120 min, respectively, and assessed by co-immunoprecipitation with a Nupr1-specific antibody, and the Nupr1-associated proteins were then probed with P-Thr/Ser, and ubiquitin antibodies, respectively. (E) Human chondrocytes were treated with 25 μM of menadione for 0 or 15 min, and assessed by co-immunoprecipitation with a Nupr1-specific antibody, and the Nupr1-associated proteins were then probed with P-Thr/Ser, and ubiquitin antibodies, respectively. Inhibitors (10 μM of p38i or 60 nM of 4μ8C) were added to the cells 1 h prior to the treatments as needed.

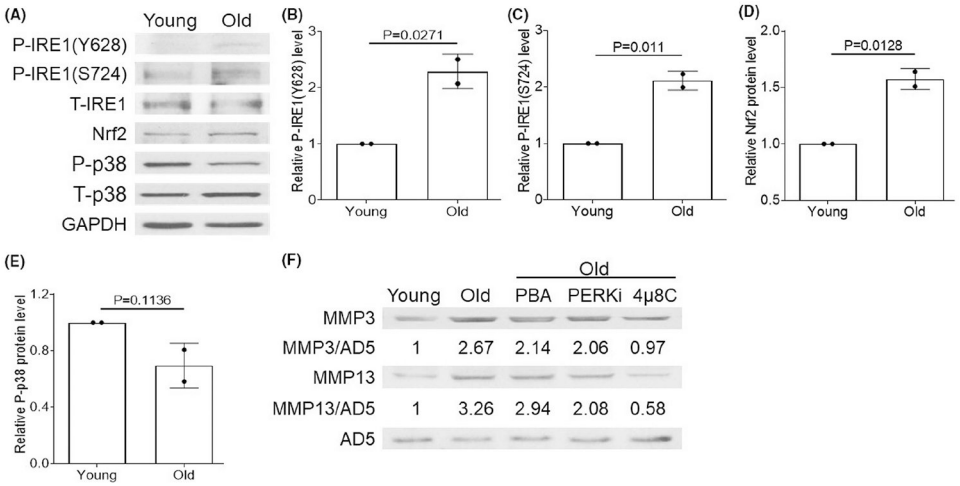

FIGURE 4.

Aging promotes both ER stress and oxidative stress to promote chondrocyte apoptosis and matrix degradation in human cartilage. (A) Chondrocytes isolated from young (<50 years of age) or old (>60 years of age) human articular cartilage were probed for P-IRE1 (Y628 or S724), T-IRE1, Nrf2, P-p38, and T-p38 antibodies, respectively. Blots were stripped and reprobed with GAPDH as a loading control. Densitometric analyses for protein levels of P-IRE1(Y628) (B), P-IRE1(S724) (C), Nrf2 (D), and P-p38 (E) were performed on blots obtained in independent experiments similar to the one shown in panel A. Data are shown as mean ± standard deviation of the mean. (F) Young or old human chondrocytes were treated with inhibitors (1 mM of PBA, 1 nM of PERKi, or 60 nM of 4μ8C overnight and then the conditioned medium was probed for MMP3 and MMP13 antibodies, respectively. Blots were stripped and reprobed with ADAMTS5 (AD5) as a loading control.

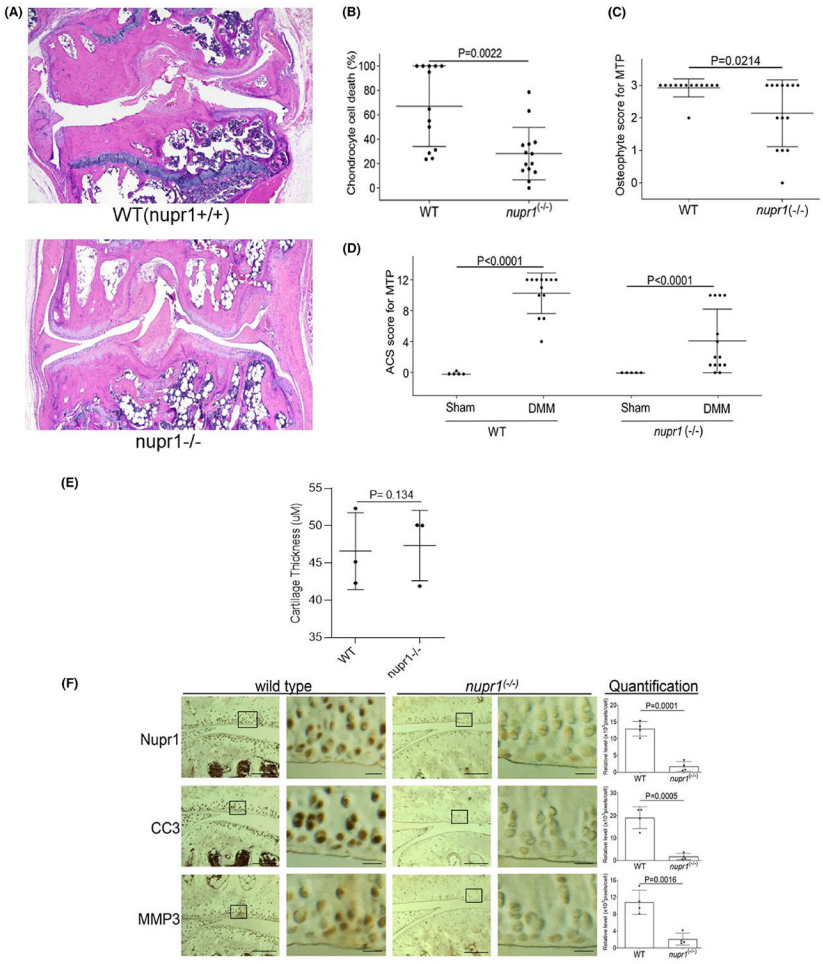

FIGURE 5.

Genetic deletion of Nupr1 reduces the severity of cartilage lesions in a mouse model of post-traumatic OA. Experimental OA was induced by DMM surgery in the left knee joints of wild-type (WT) and Nupr1$^{-/-}$ mice. After 8 weeks, knee joints were then collected, processed, and sectioned for histologic analyses. (A) Hematoxylin and eosin staining showing less OA-like changes in the knee joints of Nupr1$^{-/-}$ mice. In the WT (Nupr1$^{+/+}$) DMM mouse joint shown at the top, there is a prominent osteophyte (score = 3/3) at the medial (left) abaxial site. In the Nupr1$^{-/-}$ mouse shown below, a small osteophyte (score = 1/3) is present. (B) Percentage of area of articular cartilage occupied by dead chondrocytes. (C) Osteophyte score at the medial tibial plateau (MTP). (D) ACS score at the MTP. (E) Articular cartilage thickness is measured at the medial tibial plateau (MTP) (n = 3/genotype) as shown. (F) Mouse knee joint sections were analyzed immunohistochemically for Nupr1, CC3, and MMP3. Images on left in each set of panels are of low magnification (Scale bars: 100 μm), and the tibia is in the lower half of the images. The areas inside the small rectangles are magnified and displayed in the panels on the right (scale bars: 20 μm). All immunohistochemical data were quantified with corrections for cell numbers and statistically analyzed.

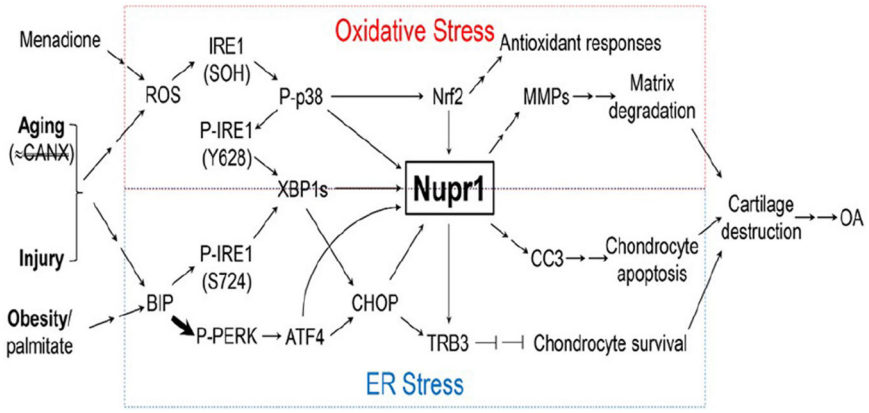

FIGURE 6.

Model showing critical role of Nupr1 in obesity, aging, and injury-linked OA pathogenesis. →, single-step stimulation; → →, multistep stimulations; big and bold arrow, dominant stimulation; ⊥ ⊥, multistep inhibitions; knockdown of calnexin; ROS, reactive oxygen species; BIP, binding immunoglobulin protein.